Effects of Al and C doping on the electronic structure and phonon renormalization in MgB_2

O. De la Peña-Seaman,[1,2] R. de Coss,[1] R. Heid,[2] and K.-P. Bohnen[2]
[1]*Departamento de Física Aplicada, Centro de Investigación y de Estudios Avanzados del IPN, Apartado Postal 73 Cordemex 97310 Mérida, Yucatán, México*
[2]*Forschungszentrum Karlsruhe, Institut für Festkörperphysik, P.O. Box 3640, D-76021 Karlsruhe, Germany*
(Received 21 January 2009; revised manuscript received 10 March 2009; published 27 April 2009)

We have studied the structural, electronic, and lattice dynamical properties of $Mg_{1-x}Al_xB_2$ and $MgB_{2(1-y)}C_{2y}$ alloys within the framework of density-functional theory using the self-consistent virtual-crystal approximation (VCA). The structural properties, electronic band structure, and full phonon dispersion have been analyzed for the $0 \leq x(\mathrm{Al}) \leq 1$ and $0 \leq y(\mathrm{C}) \leq 0.3$ ranges of concentrations. We found that both dopants reduce the number of holes in the σ bands until they are completely filled at different doping concentrations. These concentrations correlate with the experimentally observed loss of superconductivity in these alloys. The largest influence of doping on the phonon dispersion is found for the branches connected to the E_{2g} and B_{1g} modes. For both alloys a sudden increase in the E_{2g}-mode frequency is observed in a well-defined region of Al and C concentrations which correlates with the topological changes in the σ-Fermi surfaces.

DOI: 10.1103/PhysRevB.79.134523 PACS number(s): 74.25.Kc, 74.25.Jb, 74.62.Dh, 74.70.Ad

I. INTRODUCTION

Since the discovery of superconductivity in the intermetallic compound MgB_2 with a superconducting critical temperature $T_c \approx 39$ K,[1] the highest T_c for an intermetallic material, a lot of experimental and theoretical studies have been carried out in order to understand the origin of the relatively high T_c in this material. Now MgB_2 is generally accepted to be a phonon-mediated BCS-Eliashberg superconductor with multiple gaps and strong electron-phonon (e-ph) coupling.[2–6] A larger part of the coupling takes place between the σ-band Fermi surfaces (resulting from the boron p_x and p_y orbitals) with one specific phonon mode, the B-B bond stretching mode with E_{2g} symmetry at the Γ point.[4,6–10] In addition to these features, MgB_2 possesses two distinct superconducting gaps associated with the σ and π Fermi surfaces, which leads to the separation of the Eliashberg function into intra- and interband contributions.[7,11,12]

As soon as MgB_2 was discovered as a superconductor, the search for a possible family of superconductors related with it became a very active research subject. One of the first studies in this direction was the substitution of Mg by Al, where a reduction in the interplanar distance (c) and a very small change in the distance between atoms in the same plane (a) were found. However, the reduction in T_c as a function of x reported in $Mg_{1-x}Al_xB_2$ represented a more astonishing phenomena. Loss of superconductivity is found for $x > 0.5$.[13–17] The T_c reduction was successfully explained by first-principles calculations using the virtual-crystal approximation as due to filling of the σ bands with increasing x.[18] Another interesting MgB_2-based system that has received a lot of attention recently is the $MgB_{2(1-y)}C_{2y}$ alloy, which exhibits a nearly unchanged c distance, and a decrease in the a distance, in contrast to the Al-doped case. For the superconducting properties, C doping reduces T_c much faster than Al doping and suppresses superconductivity for $y > 0.15$.[19–23] The difference in the evolution of the lattice parameters between Al- and C-doped systems indicates that, although both are electron-doped systems, the doping site is crucial in determining the behavior of the different properties (structural, electronic, vibrational, and superconducting) as a function of the concentration.

The superconducting properties of MgB_2, such as the e-ph coupling and T_c, are influenced by doping in several ways. For instance, the influence could come from the changes in the chemical bond, the electronic band structure, and also the density of states, among others. Additionally, the electronic structure also influences the phonon properties such as the renormalization of the E_{2g} phonon frequency in $Mg_{1-x}Al_xB_2$. This has been demonstrated by Raman scattering measurements, which showed that the frequency increases with increasing x from ≈ 73 meV (MgB_2) to 123 meV (AlB_2).[8,24,25] Unfortunately, for the C-doped system there is no reliable phonon characterization as a function of the C content available so far. Besides the reduction of T_c with doping in $Mg_{1-x}Al_xB_2$ and $MgB_{2(1-y)}C_{2y}$, also a decrease in the superconducting gaps Δ_σ and Δ_π with $x(y)$ has been observed in these alloys. In Al-doped single crystals as well as polycrystals, it was found that the σ and π gaps do not merge even for $T_c(x \approx 0.32)$ as low as 10 K,[26–30] indicating that the interband scattering $\Gamma_{\sigma\pi}$ remains small, even at high doping levels, and is insufficient to produce the merging. For the case of the C-doped system, there are contradictory experimental results about the merging of the gaps.[27,29–33]

From the theoretical point of view, many investigations have been performed to study the evolution of the structural,[18,34] electronic,[18,35–38] vibrational,[24,39,40] and superconducting properties[36,39,41–45] of the $Mg_{1-x}Al_xB_2$ and $MgB_{2(1-y)}C_{2y}$ systems using different approximations for the simulation of the alloys, such as the supercell approach,[24,34,35,40,42] the VCA,[3,18,38,39] the coherent potential approximation (CPA),[36,37,41] and the Korringa-Kohn-Rostoker coherent potential approximation (KKR-CPA).[45] However, in particular the supercell and CPA approaches have been limited to only a few Al or C concentrations because these calculations are computationally very demanding, especially if one is interested in very low (close to Mg or B) or high concentrations (close to Al). Additionally, in these approaches the symmetry of the original system is lost,

which as a consequence complicates the interpretation and understanding of experimental results as function of doping. Finally, despite the large number of publications about MgB_2 alloys, there is so far no systematic study with *ab initio* methods covering all the different properties (starting with the structural, going through the electronic and vibrational, and ending with the electron-phonon and superconductivity parts) of both systems, $Mg_{1-x}Al_xB_2$ and $MgB_{2(1-y)}C_{2y}$.

In a previous work[18] the effects of electronic topological transitions (ETT) on the superconducting properties of the $Mg_{1-x}Al_xB_2$ alloy were analyzed. From a basic point of view, the effects of ETT on different properties (thermodynamic and kinetic) of metallic systems, produced by pressure or doping, have been studied and analyzed in the seminal paper by Lifshitz[46] several years ago. The concept of ETT has been studied in a variety of different systems and properties, such as anomalies in structural and vibrational,[47–52] thermal and transport,[53–55] and superconducting properties,[56,57] among others.

In this paper, we present a systematic study of the structural, electronic, and vibrational properties of $Mg_{1-x}Al_xB_2$ for $0.0 \leq x \leq 1.0$ and $MgB_{2(1-y)}C_{2y}$ for $0.0 \leq y \leq 0.3$ within the framework of density-functional theory[58] using the self-consistent VCA (Refs. 18 and 59–61) as implemented in the mixed-basis pseudopotential (MBPP) method.[62,63] Since it is well known that the degree of agreement with experimental results may depend on the treatment of the exchange correlation, we have used two types of *xc* functionals: the local density approximation (LDA) and the generalized gradient approximation (GGA). The calculated lattice parameters are compared with experimental data available in the literature. The evolution of the electronic band structure as a function of Al and C content is analyzed in order to determine the critical concentrations of electronic topological transitions. Vibrational properties are obtained with the linear response theory,[8,64–66] a very efficient approach implemented in the MBPP code for the calculation of lattice dynamical properties. The evolution of the phonon dispersion and the frequencies of Γ-point modes are discussed in their relation to the electronic band structure.

II. COMPUTATIONAL DETAILS

The calculations were performed with the MBPP method.[62,63] In this method, valence states are expanded in a combination of plane waves and localized functions centered at atomic sites. The latter improves the description of localized orbitals near an atomic site and allows a significant reduction in the basis set without sacrificing the accuracy. For B/C and Mg/Al norm-conserving pseudopotentials were constructed according to the description of Vanderbilt.[67] Partial core corrections have been included in all cases. The fairly deep potentials for B/C and Mg/Al are efficiently treated by the mixed-basis scheme. We used *s*- and *p*-type functions at the B/C sites, supplemented by plane waves up to a kinetic energy of 16 Ry. Phonon properties were calculated via density-functional perturbation theory[64,65] as implemented in the MBPP code.[66] The studies were carried out with two different approximations for the exchange-correlation functional, the LDA using the Hedin-Lundqvist form,[68] and the GGA using the Perdew-Burke-Ernzerhof (PBE) functional.[69–71] The Brillouin-zone integration has been performed using Monkhorst-Pack special *k*-point sets with a Gaussian smearing of 0.2 eV. For the calculation of the ground-state properties (structural optimization and elec-

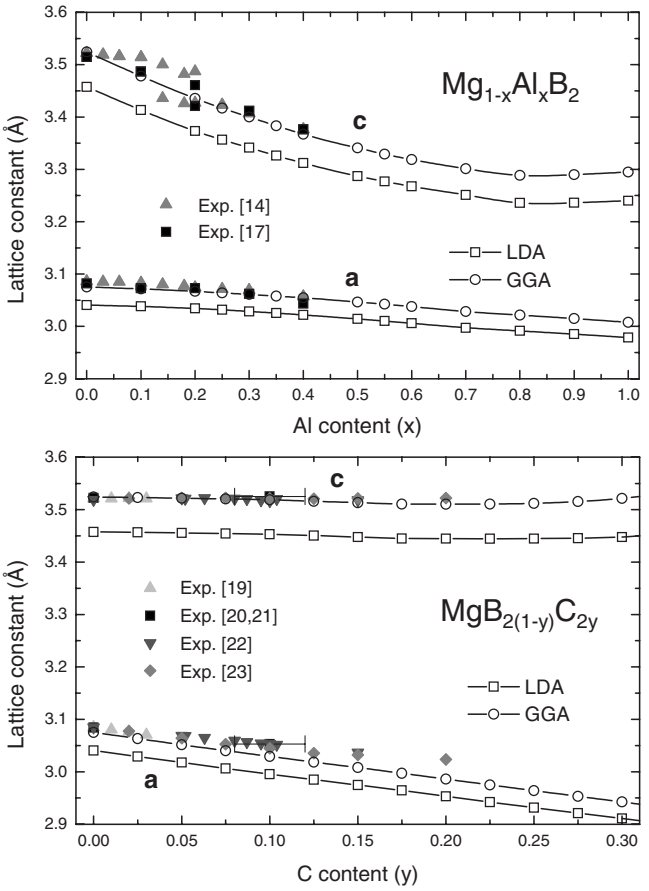

FIG. 1. Evolution of the calculated *a* and *c* lattice parameters for the $Mg_{1-x}Al_xB_2$ and $MgB_{2(1-y)}C_{2y}$ alloys, and comparison with experimental data (Refs. 14, 17, and 19–23).

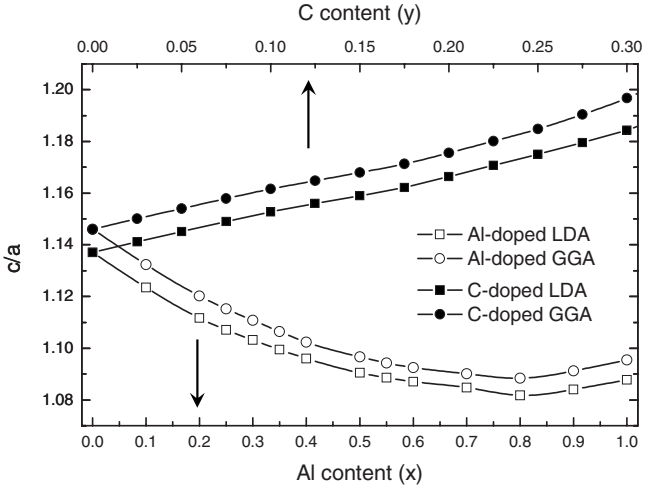

FIG. 2. Evolution of the c/a ratio for the $Mg_{1-x}Al_xB_2$ and $MgB_{2(1-y)}C_{2y}$ alloys.

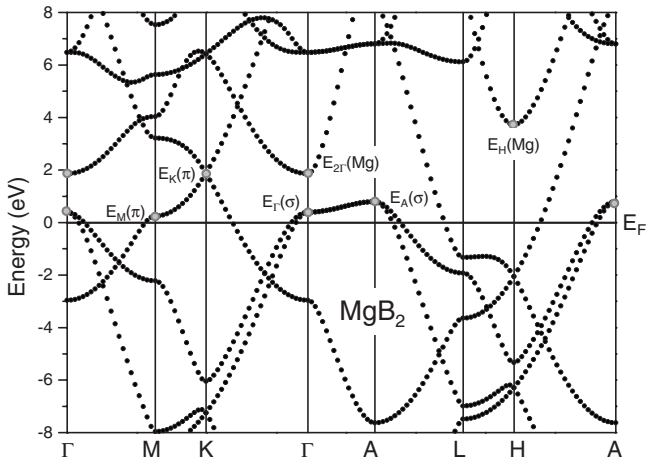

FIG. 3. Electronic band structure of MgB_2 indicating the points where electronic topological transitions can be expected with electron doping.

tronic properties) a $18\times18\times18$ k-point mesh was used while for the phonons a denser $36\times36\times36$ k-point mesh was needed for convergence.

The $Mg_{1-x}Al_xB_2$ and $MgB_{2(1-y)}C_{2y}$ alloys were modeled in the self-consistent VCA.[18,59–61,72–74] The VCA was implemented within the pseudopotential method by generating

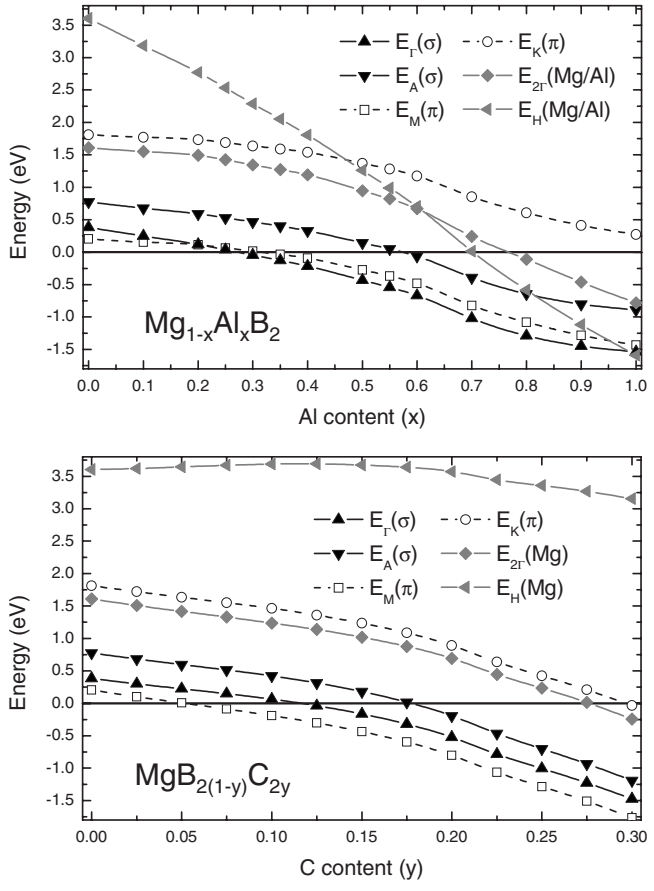

FIG. 4. Evolution of the energies corresponding to the σ, π, and (predominantly) Mg bands as a function of x for $Mg_{1-x}Al_xB_2$ and y for $MgB_{2(1-y)}C_{2y}$ alloys.

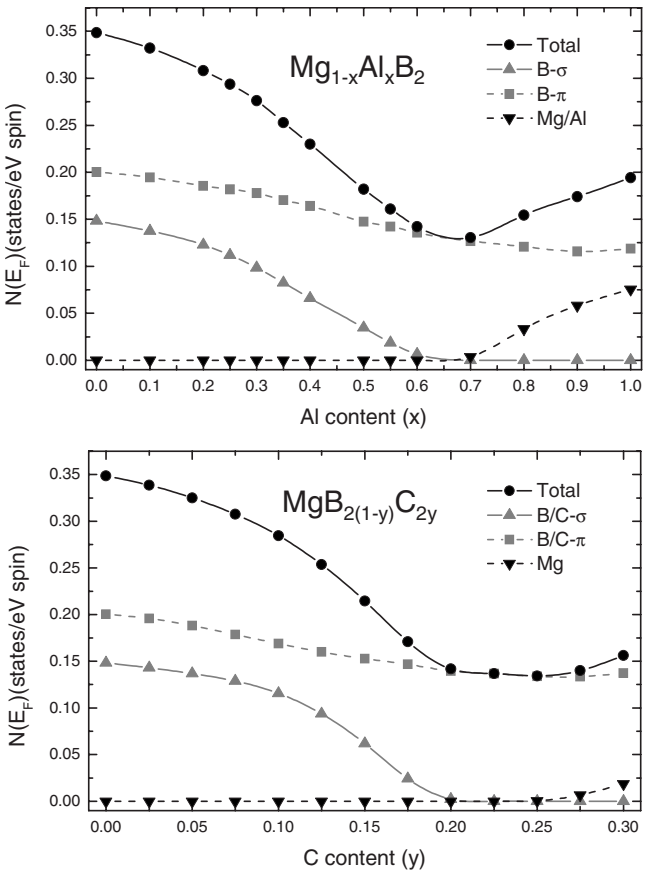

FIG. 5. Evolution of $N_i(E_F)$ ($i=\sigma$, π, Mg, and total) as a function of x for $Mg_{1-x}Al_xB_2$ and y for $MgB_{2(1-y)}C_{2y}$ alloys. The calculated values for MgB_2 are $N_\sigma=0.148$ states eV^{-1}/spin and $N_\pi=0.200$ states eV^{-1}/spin.

pseudopotentials with a fractional nuclear charge at the Mg or B site for each x and y (Al: $Z=12+x$ and C: $Z=5+y$, respectively) and by adjusting the valence charge accordingly. In previous works[60,61] the accuracy of the VCA implementation in the MBPP code has been verified by studying the structural, electronic, vibrational, and superconducting properties of the $Nb_{1-x}Mo_x$ alloys for the full range of concentra-

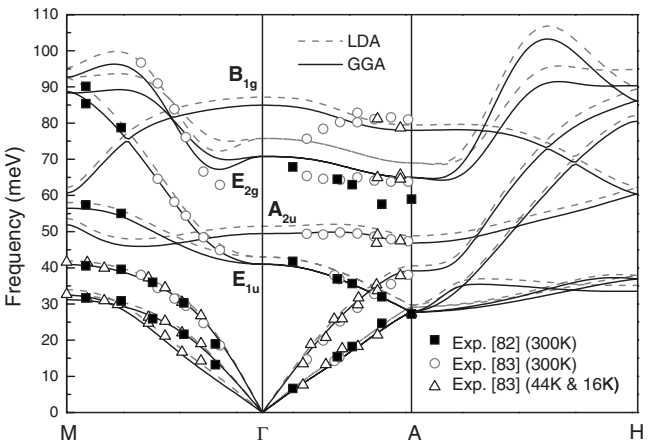

FIG. 6. Calculated and experimental (Refs. 82 and 83) phonon dispersion curves for MgB_2.

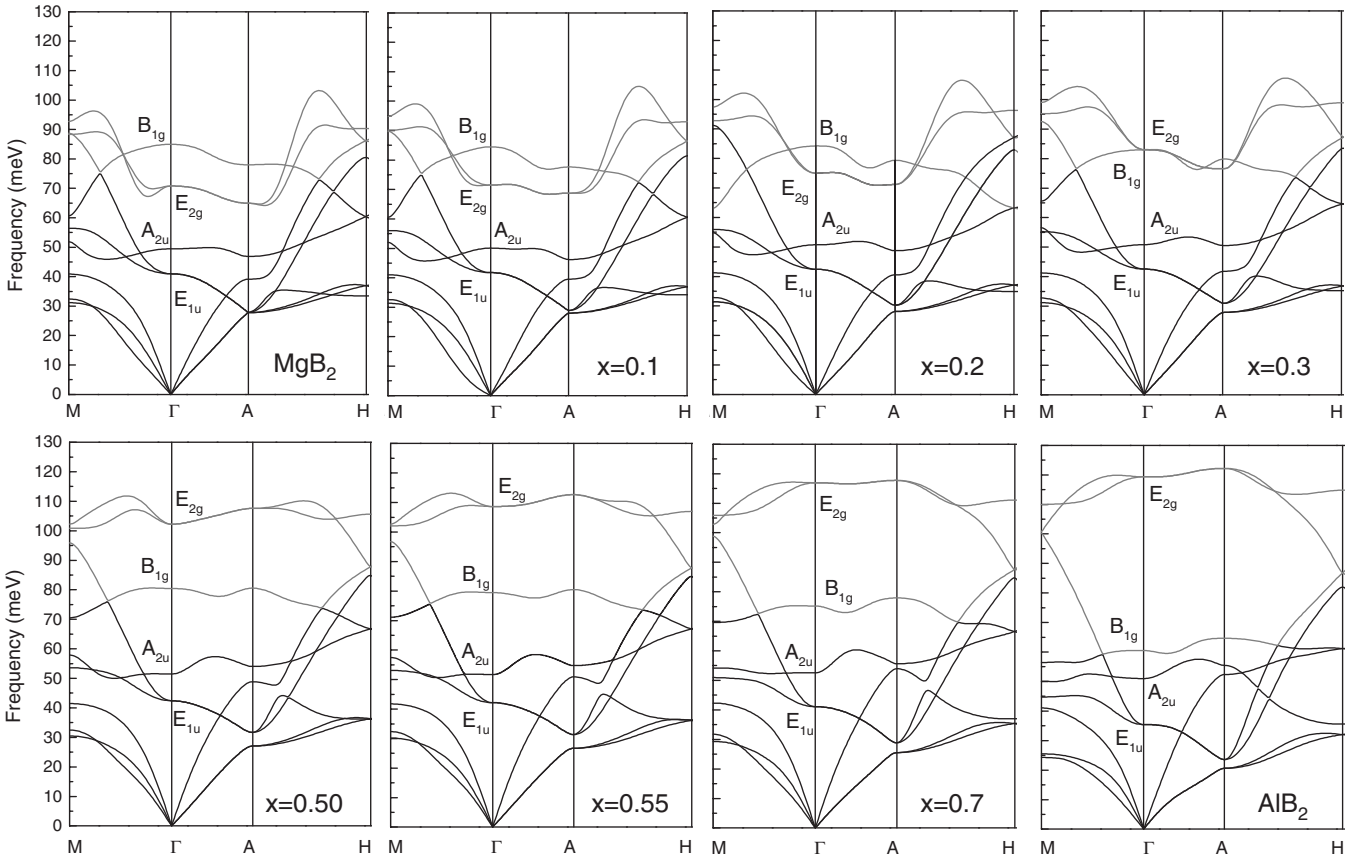

FIG. 7. Phonon dispersion of $Mg_{1-x}Al_xB_2$ as a function of x. Branches strongly affected by doping are in indicated by gray color.

tions ($0 \leq x \leq 1$) getting very good agreement with experimental results. The equilibrium lattice parameters were determined by total-energy calculations performing volume and c/a ratio variations[10] for 14 Al concentrations for $Mg_{1-x}Al_xB_2$ in the range $0 \leq x \leq 1$ and 13 C concentrations for $MgB_{2(1-y)}C_{2y}$ in the range $0 \leq y \leq 0.3$. The structural optimization was performed for both *xc* functionals: LDA and GGA.

III. RESULTS AND DISCUSSION

A. Structural properties

In Fig. 1 we show the calculated structural parameters a and c as a function of the Al and C content (x and y, respectively) in the alloys. For comparing the two systems it is worth mentioning that doping levels with equal number of excess electrons per unit cell are related by $x=2y$.

For the Al-doped system, we observe a decrease in the c lattice parameter, which is related to the interplanar distance, while the a lattice parameter, which controls the in-plane bond lengths, remains practically constant. The C-doped system shows the opposite behavior, where c is nearly constant and a decreases. This contrasting behavior can be traced back to the redistribution of the extracharge density introduced by doping. As explained in Ref. 18 for the Al-doped system, an important portion of the Al electrons is located in the interplanar region and only a small fraction in the boron planes. This leads to a strong change in the c parameter but hardly any change in a. In contrast, for the $MgB_{2(1-y)}C_{2y}$ alloy we find that the extracharge is mainly located in the area between the B atoms within the boron plane, exactly in the region of the σ bonds. This strengthens the B-B bond and, consequently, leads to a decrease in a, while it has almost no effect on the interplanar bonding and thus on c.

The calculations using the GGA *xc* functional are in better agreement with the experimental data (see Fig. 1) than LDA, in accordance with results in the literature since LDA underestimates the lattice parameters of metallic systems.[75–80] The structural optimization was also checked with the WIEN2K-LAPW method[81] (not showed here) for all concentrations. The agreement with the MBPP was excellent, independent of the *xc* functional used.

The c/a ratio for both systems given in Fig. 2 emphasizes the strong difference in the behavior of the structural parameters. In the case of Al doping, c/a decreases almost monotonically until $x \approx 0.8$ where it starts to increase again, while for the C-doped system c/a increases in a monotonic way as a function of y.

B. Electronic structure and ETT

In order to evaluate the effects of increasing the Al and C content on the electronic properties of the alloys, we analyze the evolution of the electronic band structure and the density of states at the Fermi level, $N(E_F)$. In Fig. 3 we show the band structure for MgB_2, which was calculated using GGA

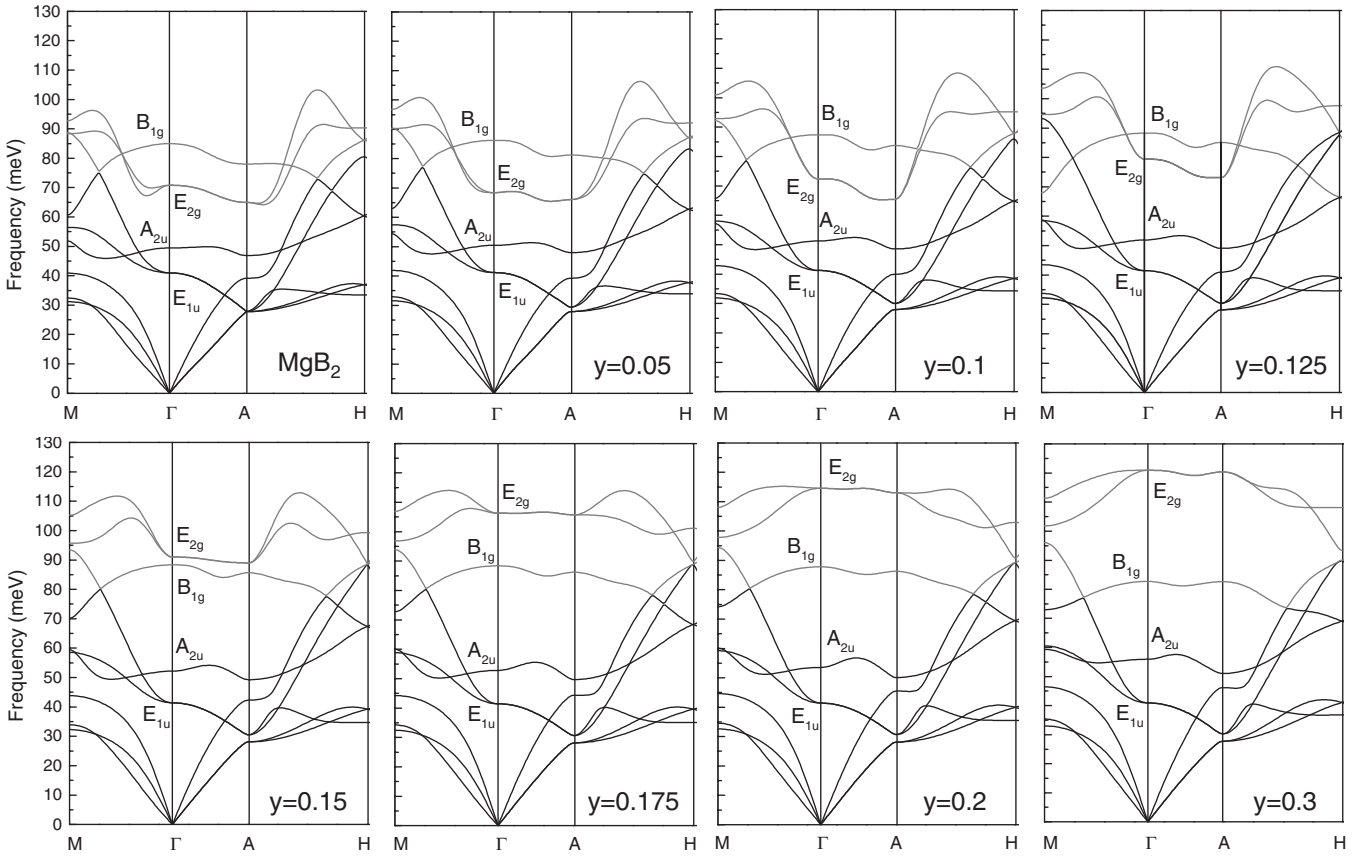

FIG. 8. Phonon dispersion of $MgB_{2(1-y)}C_{2y}$ as a function of y. Branches strongly affected by doping are in indicated by gray color.

optimized lattice parameters. In the Fig. 3, the bands are labeled where ETT with electron doping could take place.

In particular, the energies E_Γ and E_A correspond to the evolution of the σ bands, E_M and E_K trace out the evolution of the π-bands, and the energies $E_{2\Gamma}$ and E_H represent the Mg bands lying far from the Fermi level in the conduction-band region. In this way we are able to analyze the evolution of the band structure as a function of x by observing the changes in the key states of the structure: the σ and π states.

The evolution of the different band energies as a function of x and y in both systems is shown in Fig. 4 (since the LDA and GGA results are very similar in the region close to the Fermi level, we only present the latter in order to simplify the analysis). For $Mg_{1-x}Al_xB_2$ we observe that the σ bands are starting to be filled as the Al doping increases in the alloy, until E_Γ goes to zero at $x=0.27$. This represents an ETT of the σ-band Fermi surfaces and corresponds to a transition from a continuous to a discontinuous surface[18] since at Γ the semitubular Fermi surfaces collapse into one point. Increasing the Al content, the σ-band Fermi surfaces separate into disjunct pieces along the c direction, whose sizes are reduced gradually. At $x=0.57$ $E_A=0$ in the electronic band structure and the σ bands are totally filled. This vanishing of the σ-Fermi surfaces constitutes a second ETT in this band. This critical concentration, $x_c=0.57$, correlates with the loss of superconductivity in this alloy, experimentally determined at a nominal content of $x \gtrsim 0.5$.[14–17] The last result indicates that the loss of superconductivity in the $Mg_{1-x}Al_xB_2$ alloy is closely related to the filling of the σ bands of the electronic band structure.[18,44] In addition to the rapid changes in the σ bands as a function of the Al content, there are ETTs in the π bands ($E_M=0$) and also in the bands corresponding predominantly to Mg/Al states ($E_H=0$ and $E_{2\Gamma}=0$). We also studied the ETT in the $MgB_{2(1-y)}C_{2y}$ alloy. For the σ bands qualitatively the same behavior is observed as in the Al-doped system. We found the following critical values for the ETT: $E_\Gamma=0$ at $y=0.116$ and $E_A=0$ at $y=0.177$. The latter one represents the critical C content, y_c, where the σ-Fermi surfaces disappear. For comparison with the Al-doped systems these values have to be multiplied by a factor of 2 as outlined above, which leads to a critical concentration of $2y_c=0.35$. This is much smaller than for the Al-doped system ($x_c=0.57$) and indicates that the rigid band model description is inappropriate since this approximation would not differentiate between these two systems. For $MgB_{2(1-y)}C_{2y}$ the experimental value of the critical concentration where T_c goes to zero has not been reported since there are segregation problems in preparing samples of this alloy at higher C concentrations ($y>0.13$).[22,23] However, from the experimental data a loss of superconductivity is clearly observed for $y>0.15$,[19–23] which is in qualitative agreement with our value of $y_c=0.177$.

Total density of states at the Fermi energy $[N_{\text{tot}}(E_F)]$ as well as partial contributions from B-σ, B-π, and Mg states are given in Fig. 5 for both alloys as function of concentration. The σ and π partial contributions to $N_{\text{tot}}(E_F)$ for MgB_2 are $N_\sigma=0.148$ states eV^{-1}/spin and $N_\pi=0.200$ states eV^{-1}/spin, values which are very similar to those calculated

by Liu *et al.*,[11] Golubov *et al.*,[12] and Profeta *et al.*[39] The evolution of $N_i(E_F)$ ($i=\sigma$, π, Mg, and total) is very similar in both cases for the superconducting region (Al: $x \leq 0.60$; C: $y \leq 0.20$), where we observe a decrease as a function of x and y for both σ and π, with $N_\sigma(E_F)=0$ at $x_c(\mathrm{Al})=0.57$ and $y_c(\mathrm{C})=0.177$. In contrast, $N_{\mathrm{Mg}}(E_F)$ is practically zero up to $x \approx x_c$ ($y \approx y_c$) and increases for $x > x_c$ ($y > y_c$) in both cases. This upturn at higher doping levels is more pronounced for Al than for C doping.

C. Lattice dynamics

In this subsection we discuss the vibrational properties of the Al- and C-doped MgB_2 alloys. In Fig. 6 we show the phonon dispersion for MgB_2 calculated within LDA and GGA, respectively, in comparison with experimental data available in the literature.[82,83] While both calculations agree rather well with the experimental data, GGA (black solid lines) performs slightly better than LDA (gray dotted lines). Therefore, we restrict further analysis to the GGA case.

For the alloys we have obtained the full phonon dispersion curves for ten Al as well as ten C concentrations. The results for $Mg_{1-x}Al_xB_2$ and $MgB_{2(1-y)}C_{2y}$ alloys are given in Figs. 7 and 8, respectively (showing the most representative results). The B_{1g} and E_{2g} branches, which are most strongly affected by doping, are marked with gray color in both figures. As a general trend for both alloys, we observe a hardening of the E_{2g} branches as well as a softening of the B_{1g} branch with increasing doping. This leads to a rather flat dispersion of the E_{2g} branches for larger doping [$x(\mathrm{Al}) \gtrsim 0.55$ and $y(\mathrm{C}) \gtrsim 0.177$]. The B_{1g} branch initially softens only slightly for both alloys, but in the case of $Mg_{1-x}Al_xB_2$, a pronounced frequency reduction occurs close to $x=1$.

To discuss the doping related effects in more detail we now focus our attention on the B_{1g} and E_{2g} modes at the Γ point. We show in Fig. 9 their phonon frequencies as a function of x for $Mg_{1-x}Al_xB_2$ and y for $MgB_{2(1-y)}C_{2y}$ alloys.[84] Three different regimes can be distinguished for the E_{2g} mode. For small doping (Al: $0 \leq x \leq 0.25$; C: $0 \leq x \leq 0.10$) the E_{2g} frequency increases very slightly for the Al doping and stays almost constant for the case of C doping. For intermediate doping (Al: $0.25 \leq x \leq 0.60$; C: $0.10 \leq y \leq 0.20$) there is a strong increase in the frequency as a function of x and y. This effect is more pronounced for C doping since the transition region is narrower than in the Al-doped system. The region where the hardening happens correlates closely with the range of concentrations between the two ETTs of the σ bands, which indicate a change in the topology ($E_\Gamma=0$) and the complete disappearance of the σ-Fermi surfaces ($E_A=0$), respectively. As soon as the number of empty σ states (holes) starts to decrease due to Al or C doping (electrons), the scattering channel responsible for the huge phonon renormalization in MgB_2 is partly closed leading to a reduced renormalization and thus to an increased frequency for the E_{2g} mode. Finally, the large doping regime (Al: $0.60 \leq x \leq 1$; C: $0.20 \leq y \leq 0.30$) shows a saturation of the E_{2g} frequency. The B_{1g} mode behaves qualitatively different for the two alloys. It decreases in a monotonic way for Al doped while staying nearly constant for the C-doped system.

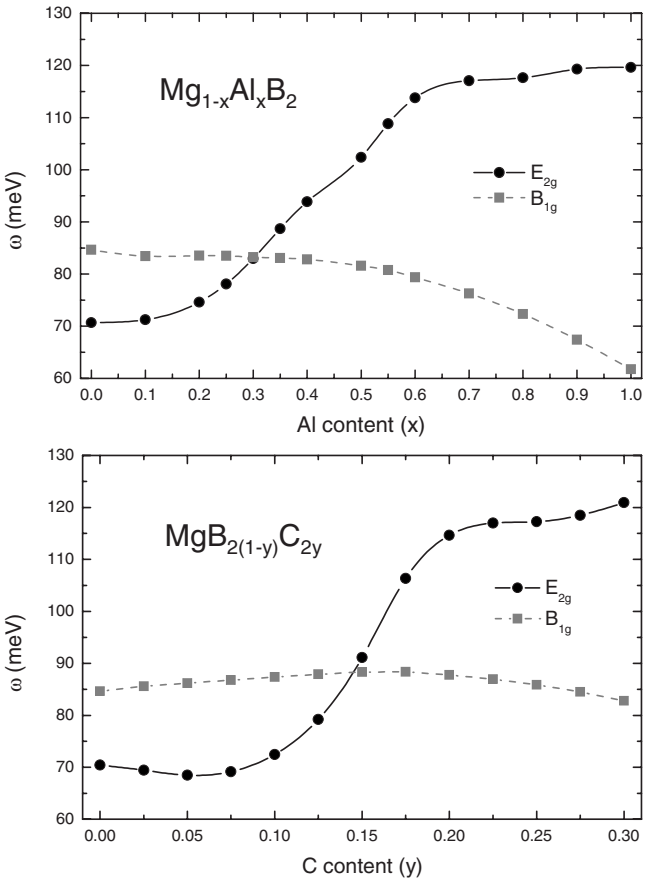

FIG. 9. Evolution of the E_{2g}- and B_{1g}-phonon mode frequencies at Γ as a function of x for $Mg_{1-x}Al_xB_2$ and y for $MgB_{2(1-y)}C_{2y}$ alloys.

The reason for this different behavior is that for the Al doping the extracharge is located in the interplanar region,[18] which affects in a direct way the buckling-type B_{1g} mode. For the C-doped system, the charge density in this region is practically unchanged since almost all the extracharges are located in the boron plane.

IV. CONCLUSIONS

We have performed a first-principles study of the structural parameters, the electronic structure, and the vibrational properties for the $Mg_{1-x}Al_xB_2$ and $MgB_{2(1-y)}C_{2y}$ alloys as a function of x and y, respectively, using the self-consistent virtual-crystal approximation. We find very good agreement with experimental results for the structural properties in both cases, indicating that VCA works well in describing these alloy systems. Both systems exhibit five electronic topological transitions, corresponding to the σ, π, and Mg/Al bands. The first critical concentration for the σ bands, $x_1(\mathrm{Al})=0.27$ and $y_1(\mathrm{C})=0.116$, corresponds to a disruption of the tubular structure of the Fermi surface at the Γ point. The second one, $x_2(\mathrm{Al})=0.57$ and $y_2(\mathrm{C})=0.177$, corresponds to the complete filling of the σ bands. The latter ones correlate with the concentrations where superconductivity disappears in these alloys. The calculated phonon dispersion for MgB_2

is in good agreement with the experimental data available in the literature. In particular, GGA performs better than LDA. The frequency of the B_{1g} mode monotonically decreases for Al doping, while it stays nearly constant for the C-doped system. This qualitatively different behavior reflects the sensitivity of this mode to the region in the unit cell where the extracharge is located. Finally, the E_{2g} mode shows an abrupt renormalization loss (hardening) in a well-defined range of Al and C concentrations. This transition region correlates with the range between the two ETTs of the σ bands, indicating the strong influence of the electronic structure in determining the vibrational properties of these alloys.

The successful application of the self-consistent virtual-crystal approximation to electronic and vibrational properties on these alloys opens the way for a first-principles investigation of electron-phonon coupling and superconducting properties as a function of doping, a study that will be the topic of a forthcoming paper.[85]

ACKNOWLEDGMENTS

This research was supported by the Consejo Nacional de Ciencia y Tecnología (CONACYT), México under Grant No. 43830-F and the Forschungszentrum Karlsruhe, Germany. One of the authors (O.P.-S.) gratefully acknowledges a student award from CONACYT-México and the support from the Forschungszentrum Karlsruhe and the Gobierno del Estado de Yucatán, México.

[1] J. Nagamatsu, N. Nakagawa, T. Muranaka, Y. Zanitai, and J. Akimitsu, Nature (London) **410**, 63 (2001).
[2] J. M. An and W. E. Pickett, Phys. Rev. Lett. **86**, 4366 (2001).
[3] J. Kortus, I. I. Mazin, K. D. Belashchenko, V. P. Antropov, and L. L. Boyer, Phys. Rev. Lett. **86**, 4656 (2001).
[4] A. Q. R. Baron, H. Uchiyama, S. Tsutsui, Y. Tanaka, D. Ishikawa, J. P. Sutter, S. Lee, S. Tajima, R. Heid, and K. P. Bohnen, Physica C **456**, 83 (2007).
[5] A. Floris, A. Sanna, M. Lüders, G. Profeta, N. N. Lathiotakis, M. A. L. Marques, C. Franchini, E. K. U. Gross, A. Continenza, and S. Massidda, Physica C **456**, 45 (2007).
[6] J. Kortus, Physica C **456**, 54 (2007).
[7] Y. Kong, O. V. Dolgov, O. Jepsen, and O. K. Andersen, Phys. Rev. B **64**, 020501(R) (2001).
[8] K. P. Bohnen, R. Heid, and B. Renker, Phys. Rev. Lett. **86**, 5771 (2001).
[9] T. Yildirim, O. Gulseren, J. W. Lynn, C. M. Brown, T. J. Udovic, Q. Huang, N. Rogado, K. A. Regan, M. A. Hayward, J. S. Slusky, T. He, M. K. Haas, P. Khalifah, K. Inumaru, and R. J. Cava, Phys. Rev. Lett. **87**, 037001 (2001).
[10] K. Kunc, I. Loa, K. Syassen, R. K. Kremer, and K. Ahn, J. Phys.: Condens. Matter **13**, 9945 (2001).
[11] A. Y. Liu, I. I. Mazin, and J. Kortus, Phys. Rev. Lett. **87**, 087005 (2001).
[12] A. A. Golubov, J. Kortus, O. V. Dolgov, O. Jepsen, Y. Kong, O. K. Andersen, B. J. Gibson, K. Ahn, and R. K. Kremer, J. Phys.: Condens. Matter **14**, 1353 (2002).
[13] J. Geerk, R. Schneider, G. Linker, A. G. Zaitsev, R. Heid, K. P. Bohnen, and H. v. Löhneysen, Phys. Rev. Lett. **94**, 227005 (2005).
[14] J. S. Slusky, N. Rogado, K. A. Regan, M. A. Hayward, P. Khalifah, T. He, K. Inumaru, S. M. Loureiro, M. K. Hass, H. W. Zandbergen, and R. J. Cava, Nature (London) **410**, 343 (2001).
[15] A. Bianconi, D. Di Castro, S. Agrestini, G. Campi, N. L. Saini, A. Saccone, S. De Negri, and M. Giovannini, J. Phys.: Condens. Matter **13**, 7383 (2001).
[16] P. Postorino, A. Congeduti, P. Dore, A. Nucara, A. Bianconi, D. Di Castro, S. De Negri, and A. Saccone, Phys. Rev. B **65**, 020507(R) (2001).
[17] H. D. Yang, H. L. Liu, J. Y. Lin, M. X. Kuo, P. L. Ho, J. M. Chen, C. U. Jung, M. S. Park, and S. I. Lee, Phys. Rev. B **68**, 092505 (2003).
[18] O. de la Pena, A. Aguayo, and R. de Coss, Phys. Rev. B **66**, 012511 (2002).
[19] T. Takenobu, T. Ito, D. H. Chi, K. Prassides, and Y. Iwasa, Phys. Rev. B **64**, 134513 (2001).
[20] R. A. Ribeiro, S. L. Bud'ko, C. Petrovic, and P. C. Canfield, Physica C **384**, 227 (2003).
[21] M. Avdeev, J. D. Jorgensen, R. A. Ribeiro, S. L. Bud'ko, and P. C. Canfield, Physica C **387**, 301 (2003).
[22] S. M. Kazakov, J. Karpinski, J. Jun, P. Geiser, N. D. Zhigadlo, R. Puzniak, and A. V. Mironov, Physica C **408-410**, 123 (2004).
[23] S. Lee, T. Masui, A. Yamamoto, H. Uchiyama, and S. Tajima, Physica C **397**, 7 (2003).
[24] B. Renker, K. B. Bohnen, R. Heid, D. Ernst, H. Schober, M. Koza, P. Adelmann, P. Schweiss, and T. Wolf, Phys. Rev. Lett. **88**, 067001 (2002).
[25] D. Di Castro, S. Agrestini, G. Campi, A. Cassetta, M. Colapietro, A. Congeduti, A. Continenza, S. De Negri, M. Giovannini, S. Massidda, M. Nardone, A. Pifferi, P. Postorino, G. Profeta, A. Saccone, N. L. Saini, G. Satta, and A. Bianconi, Europhys. Lett. **58**, 278 (2002).
[26] R. S. Gonnelli, D. Daghero, A. Calzolari, G. A. Ummarino, V. Dellarocca, V. A. Stepanov, S. M. Kazakov, N. Zhigadlo, and J. Karpinski, Phys. Rev. B **71**, 060503(R) (2005).
[27] D. Daghero, D. Delaude, A. Calzolari, M. Tortello, G. A. Ummarino, R. S. Gonnelli, V. A. Stepanov, N. D. Zhigadlo, S. Katrych, and J. Karpinski, J. Phys.: Condens. Matter **20**, 085225 (2008).
[28] T. Klein, L. Lyard, J. Marcus, C. Marcenat, P. Szabó, Z. Hol'anová, P. Samuely, B. W. Kang, H. J. Kim, H. S. Lee, H. K. Lee, and S. I. Lee, Phys. Rev. B **73**, 224528 (2006).
[29] P. Szabó, P. Samuely, Z. Pribulová, M. Angst, S. Bud'ko, P. C. Canfield, and J. Marcus, Phys. Rev. B **75**, 144507 (2007).
[30] R. S. Gonnelli, D. Daghero, G. A. Ummarino, M. Tortello, D. Delaude, V. A. Stepanov, and J. Karpinski, Physica C **456**, 134 (2007).
[31] H. Schmidt, J. F. Zasadzinski, K. E. Gray, and D. G. Hinks, Phys. Rev. Lett. **88**, 127002 (2002).
[32] Z. Hol'anová, P. Szabó, P. Samuely, R. H. T. Wilke, S. L. Bud'ko, and P. C. Canfield, Phys. Rev. B **70**, 064520 (2004).
[33] S. Tsuda, T. Yokoya, T. Kiss, T. Shimojima, S. Shin, T. Togashi,

S. Watanabe, C. Zhang, C. T. Chen, S. Lee, H. Uchiyama, S. Tajima, N. Nakai, and K. Machida, Phys. Rev. B **72**, 064527 (2005).
[34] S. V. Barabash and D. Stroud, Phys. Rev. B **66**, 012509 (2002).
[35] S. Suzuki, S. Higai, and K. Nakao, J. Phys. Soc. Jpn. **70**, 1206 (2001).
[36] P. P. Singh, Solid State Commun. **127**, 271 (2003).
[37] D. Kasinathan, K. W. Lee, and W. E. Pickett, Physica C **424**, 116 (2005).
[38] L. D. Cooley, A. J. Zambano, A. R. Moodenbaugh, R. F. Klie, J. C. Zheng, and Y. Zhu, Phys. Rev. Lett. **95**, 267002 (2005).
[39] G. Profeta, A. Continenza, and S. Massidda, Phys. Rev. B **68**, 144508 (2003).
[40] A. H. Moudden, J. Phys. Chem. Solids **88**, 067001 (2006).
[41] P. P. Singh, Physica C **382**, 381 (2002).
[42] A. Bussmann-Holder and A. Bianconi, Phys. Rev. B **67**, 132509 (2003).
[43] G. A. Ummarino, R. S. Gonnelli, and A. Bianconi, J. Supercond. Novel Magn. **18**, 791 (2005).
[44] J. Kortus, O. V. Dolgov, R. K. Kremer, and A. A. Golubov, Phys. Rev. Lett. **94**, 027002 (2005).
[45] P. J. T. Joseph and P. P. Singh, Physica C **454**, 43 (2007).
[46] I. M. Lifshitz, Sov. Phys. JETP **11**, 1130 (1960).
[47] V. G. Vaks and A. V. Trefilov, J. Phys.: Condens. Matter **3**, 1389 (1991).
[48] V. G. Vaks, M. I. Katsnelson, A. I. Likhtenstein, G. V. Peschanskikh, and A. V. Trefilov, J. Phys.: Condens. Matter **3**, 1409 (1991).
[49] E. Bruno, B. Ginatempo, and E. S. Giuliano, Phys. Rev. B **52**, 14544 (1995).
[50] E. Bruno, B. Ginatempo, and E. S. Giuliano, Phys. Rev. B **52**, 14557 (1995).
[51] B. Magyari-Kope, G. Grimvall, and L. Vitos, Phys. Rev. B **66**, 064210 (2002).
[52] N. I. Medvedeva, Y. N. Gornostyrev, and A. J. Freeman, Phys. Rev. B **67**, 134204 (2003).
[53] W. H. Butler and G. M. Stocks, Phys. Rev. B **29**, 4217 (1984).
[54] J. C. Swihart, W. H. Butler, G. M. Stocks, D. M. Nicholson, and R. C. Ward, Phys. Rev. Lett. **57**, 1181 (1986).
[55] D. L. Novikov, M. I. Katsnelson, A. V. Trefilov, A. J. Freeman, N. E. Christensen, A. Svane, and C. O. Rodriguez, Phys. Rev. B **59**, 4557 (1999).
[56] V. I. Makarov and V. G. Bar'yakhtar, Sov. Phys. JETP **21**, 1151 (1965).
[57] D. L. Novikov and A. J. Freeman, Physica C **216**, 273 (1993).
[58] J. W. Kohn and L. J. Sham, Phys. Rev. **140**, A1133 (1965).
[59] M. J. Mehl, D. A. Papaconstantopoulos, and D. J. Singh, Phys. Rev. B **64**, 140509(R) (2001).
[60] O. De la Peña-Seaman, R. de Coss, R. Heid, and K. P. Bohnen, Phys. Rev. B **76**, 174205 (2007).
[61] O. De la Peña-Seaman, R. de Coss, R. Heid, and K. P. Bohnen, J. Phys.: Condens. Matter **19**, 476216 (2007).
[62] S. G. Louie, K. M. Ho, and M. L. Cohen, Phys. Rev. B **19**, 1774 (1979).
[63] B. Meyer, C. Elsässer, and M. Fähnle, FORTRAN90 Program for Mixed-Basis Pseudopotential Calculations for Crystals, Max-Planck-Institut fur Metallforschung, Stuttgart (unpublished).
[64] S. Baroni, P. Giannozzi, and A. Testa, Phys. Rev. Lett. **58**, 1861 (1987).
[65] P. Giannozzi, S. de Gironcoli, P. Pavone, and S. Baroni, Phys. Rev. B **43**, 7231 (1991).
[66] R. Heid and K. P. Bohnen, Phys. Rev. B **60**, R3709 (1999).
[67] D. Vanderbilt, Phys. Rev. B **32**, 8412 (1985).
[68] L. Hedin and B. I. Lundqvist, J. Phys. C **4**, 2064 (1971).
[69] V. Ozolins and M. Korling, Phys. Rev. B **48**, 18304 (1993).
[70] K. Kokko and M. P. Das, J. Phys.: Condens. Matter **10**, 1285 (1998).
[71] J. P. Perdew, K. Burke, and M. Ernzerhof, Phys. Rev. Lett. **77**, 3865 (1996).
[72] D. A. Papaconstantopoulos, E. N. Economou, B. M. Klein, and L. L. Boyer, Phys. Rev. B **20**, 177 (1979).
[73] C. Ambrosch-Draxl, P. Sule, H. Auer, and E. Y. Sherman, Phys. Rev. B **67**, 100505(R) (2003).
[74] T. Thonhauser and C. Ambrosch-Draxl, Phys. Rev. B **67**, 134508 (2003).
[75] A. Dal Corso, A. Pasquarello, A. Baldereschi, and R. Car, Phys. Rev. B **53**, 1180 (1996).
[76] J. E. Jaffe, Z. Lin, and A. C. Hess, Phys. Rev. B **57**, 11834 (1998).
[77] C. Stampfl and C. G. Van de Walle, Phys. Rev. B **59**, 5521 (1999).
[78] F. Favot and A. Dal Corso, Phys. Rev. B **60**, 11427 (1999).
[79] C. Stampfl, W. Mannstadt, R. Asahi, and A. J. Freeman, Phys. Rev. B **63**, 155106 (2001).
[80] A. Janotti, S. H. Wei, and D. J. Singh, Phys. Rev. B **64**, 174107 (2001) ISBN 3–9501031–1–2.
[81] P. Blaha, K. Schwarz, G. K. H. Madsen, D. Kvasnicka, and J. Luitz, *WIEN2K, An Augmented Plane Wave + Local Orbitals Program for Calculating Crystal Properties* (Karlheinz Schwarz, Techn. Universität Wien, Austria, 2001) ISBN 3–9501031–1–2.
[82] A. Shukla *et al.*, Phys. Rev. Lett. **90**, 095506 (2003).
[83] A. Q. R. Baron, H. Uchiyama, Y. Tanaka, S. Tsutsui, D. Ishikawa, S. Lee, R. Heid, K. P. Bohnen, S. Tajima, and T. Ishikawa, Phys. Rev. Lett. **92**, 197004 (2004).
[84] Experimental data are not included because available Raman measurements are not conclusive due to the existence of two peaks in the spectra (Refs. 8, 24, and 25).
[85] O. De la Peña-Seaman, R. de Coss, R. Heid, and K. P. Bohnen (to be published).